Supercurrents through *SNS* proximity-induced junctions

Herman J. Fink
Department of Electrical and Computer Engineering, University of California, Davis, California 95616
(Received 24 September 1996; revised manuscript received 7 January 1997)

Critical current measurements by Courtois *et al.* [Phys. Rev. B **52**, 1162 (1995)] on proximity-induced superconductivity in a narrow metallic wire are analyzed by a junction model of the author based on the Ginzburg-Landau theory. Good agreement is found if one assumes that the length of at least one of the many superconducting cells is larger than anticipated by a factor of approximately 2. At low temperatures the size of the superconducting region in the normal metal is confined by the length of the normal cell. As a consequence, the critical current saturates below a temperature at which the length of the normal cell becomes approximately three characteristic lengths of the coherent state in the normal metal. [S0163-1829(97)03429-2]

Courtois *et al.*[1] investigated experimentally proximity-induced superconductivity in narrow metallic wires of Cu and Ag. Figure 1 shows the experimental arrangement of superconducting (Al) and normal conducting (Cu, Ag) wires. The measuring current is passed along the Cu or Ag wire. The total length of the normal conducting wire is given as 76.8 μm and the spacing of the superconducting wires as 0.8 μm for the Ag-Al specimen 17, a typical specimen. It is possible that there could have been up to 96 superconducting Al branches connected to the silver wire. One of the sensitive parameters which determines the value of the critical current of the Ag branches is the distance between the proximity-induced patches located on the Ag wire underneath the Al branches, that is, the distance $(d-w_s)$. If one of the Al branches does not make electrical contact with the Ag wire, then the effective distance is equal to $(2d-w_s)$, and it is this latter distance which would then determine the critical current of the silver wire.

When comparing experiment[1] with theory,[2] the authors did not obtain agreement with de Gennes' superconducting–normal-metal–superconducting (*SNS*) equation, and consequently concluded that their ''study of the low-temperature zero-resistance state shows a purely new behavior that is definitely out of the scope of classical *SNS* junctions models.''

As pointed out by Yamafuji *et al.*,[3] the boundary condition at the *SN* interface as used in Ref. 2 leads to a discontinuous phase current across the boundaries. These shortcomings have been eliminated in Refs. 4 and 5, and the theory has been generalized to arbitrary mean free paths of the *S* and *N* metal as well as extended to SS_1S junctions, where S_1 is a superconductor different from *S*. The results of Ref. 4 have been used previously to describe successfully critical current measurements on SNS junctions by Clarke.[6]

Although it is possible to start, with the approximate result, Eq. (31) of Ref. 4, to unravel the results of Ref. 1, we find it didactic to outline the derivation of an exact solution in order to show where inaccuracies and uncertainties might arise in the theory.

The relation between the *modulus* of the order parameter $F(x,T)$ and the pair potential Δ_{Gs} for a superconductor is[7,8]

$$F_s=\left[\frac{7}{8}\zeta(3)n_s\chi_{Gs}\right]^{1/2}(|\Delta_{Gs}|/\pi kT_c), \tag{1}$$

where n_s is the total electron density of the superconductor, $\chi_{Gs}(\xi_0,l_s)$ is a function of the intrinsic (BCS) coherence length ξ_0 and the mean free path l_s, k is Boltzmann's constant, and T_c is the transition temperature of the superconductor.

Superconductivity in the *N* region depends entirely on the inherent superconductivity of the *S* region. It is therefore reasonable to assume that the coherent state in the *N* region will exist only below T_c of the *S* region. Furthermore, it is then reasonable to normalize all properties in the *N* region by the same normalization factor as is applied to the *S* region. For the *N* region we postulate an equation similar to Eq. (1):

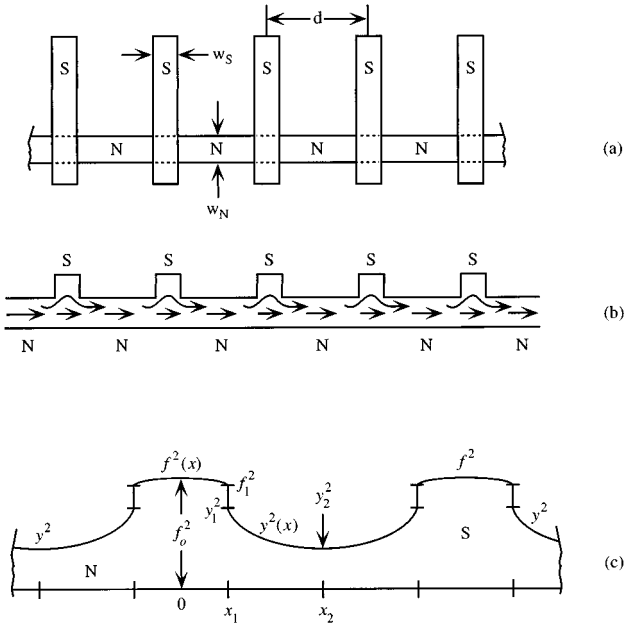

FIG. 1. (a) A narrow Ag wire, length 76.8 μm, is covered with superconducting (Al) branches, distance $d=0.8$ μm apart. Ag width $w_N=0.21$ μm, Ag thickness $e_N=0.15$ μm, Al width $w_S=0.12$ μm. There is no current injected through the Al branches. Current flows through the continuous Ag wire. Superconductivity is induced in the Ag wire at the site where Al makes electrical contact (from Ref. 1). (b) Side view of (a) with current flow indicated. (c) Schematic of functions represented by Eqs. (10) and (13).

$$F_n=\left[\frac{7}{8}\zeta(3)n_n\chi_{Gn}\right]^{1/2}(|\Delta_{Gn}|/\pi kT_c), \tag{2}$$

where n_n is the total electron density of the N metal, $\chi_{Gn}(|\xi_n|,l_n)$ is a function of the characteristic length $|\xi_n(T)|$ of the coherent state in the N metal, and l_n is the mean free path in the N region. T_c is that of the superconductor. Normalizing Eq. (1) by the S region bulk values and Eq. (2) by

$$F_n^2(\infty)=F_s^2(\infty)(n_n/n_s)(\chi_{Gn}/\chi_{Gs}), \tag{3}$$

one obtains

$$f(x,T)=F_s/F_s(\infty)=|\Delta_{Gs}|/|\Delta_{Gs}(\infty)|, \tag{4}$$

$$y(x,T)=F_n/F_n(\infty)=|\Delta_{Gn}|/|\Delta_{Gs}(\infty)|, \tag{5}$$

which satisfy the following differential equations[4] in one dimension:

$$(\xi_s(T))^2\frac{d^2f}{dx^2}+\left(1-f^2-\frac{i^2}{f^4}\right)f=0 \quad \text{in the } S \text{ region}, \tag{6}$$

$$-|\xi_n(T)|^2\frac{d^2y}{dx^2}+\left(1-y^2+\frac{I^2}{y^4}\right)y=0 \quad \text{in the } N \text{ region}, \tag{7}$$

where i is the normalized current density in the S region: $i=(\lambda_s/\sqrt{2}H_c)J$. The current density J is in mks units with $H_c(T)$, the thermodynamic critical field, in A/m, and $\lambda_s(T)$ is the Ginzburg-Landau penetration depth of the superconductor. The symbol I in Eq. (7) is the normalized current density in the N region and is defined by

$$I=\frac{|\xi_n|}{\xi_s}\frac{m_n}{m_s}\frac{n_s}{n_n}\frac{\chi_{Gs}}{\chi_{Gn}}i. \tag{8}$$

In the ''one-dimensional'' case, with equal cross-sectional area of the wires, the real current density J must be the same in the S and N regions.

Equation (6) is the one-dimensional Ginzburg-Landau equation, while Eq. (7) is a distinctly different differential equation. In principle, both equations can be solved exactly. The solutions are

$$\xi_s^2\left(\frac{df^2}{dx}\right)^2=2(f_0^2-f^2)\left[f^2(2-f_0^2-f^2)-\frac{2i^2}{f_0^2}\right], \tag{9}$$

$$f^2=f_0^2-a_s^2m_s\mathrm{sd}^2(u_s|m_s). \tag{10}$$

f_0 is the value of $f(x,T)$ at its maximum as shown in Fig. 1(c). a_s, m_s, and u_s are functions of f_0, T and i, and are

$$S_s=1-3f_0^2/2,$$

$$R_s=[(1-f_0^2/2)^2-2i^2/f_0^2]^{1/2},$$

$$a_s^2=S_s+R_s,$$

$$b_s^2=-S_s+R_s,$$

$$m_s=b_s^2/(a_s^2+b_s^2),$$

$$u_s=[(a_s^2+b_s^2)/2]^{1/2}x/\xi_s(T). \tag{11}$$

Similarly, Eq. (7) can be solved exactly with solutions:

$$|\xi_n|^2\left(\frac{dy^2}{dx}\right)^2=2(y^2-y_2^2)\left[y^2(2-y_2^2-y^2)+\frac{2I^2}{y_2^2}\right], \tag{12}$$

$$y^2=y_2^2+a_n^2m_n\mathrm{sd}^2(u_n|m_n), \tag{13}$$

where y_2 is the value of $y(x,T)$ at the minimum in the N region and a_n, m_n, and u_n are functions of y_2, T, and I, defined by

$$S_n=1-3y_2^2/2,$$

$$R_n=[(1-y_2^2/2)^2+2I^2/y_2^2]^{1/2},$$

$$a_n^2=-S_n+R_n,$$

$$b_n^2=+S_n+R_n,$$

$$m_n=b_n^2/(a_n^2+b_n^2),$$

$$u_n=[(a_n^2+b_n^2)/2]^{1/2}|x-x_2|/|\xi_n(T)|. \tag{14}$$

Although Eqs. (10) and (13) are similar in form, they are distinctly different. They cannot be transformed into each other (in form) by a translation of the coordinate system.

As in a superconducting micronetwork,[9] continuity of the phase current requires that

$$m_s^{-1}dF_s^2/dx=m_n^{-1}dF_n^2/dx$$

at the SN interface. From this it follows that the following condition must be satisfied:

$$\left.\frac{dy^2}{dx}\right|_{x_1}=\frac{m_n}{m_s}\frac{n_s}{n_n}\frac{\chi_{Gs}}{\chi_{Gn}}\left.\frac{df^2}{dx}\right|_{x_1}. \tag{15}$$

Furthermore, there may be an apparent or real discontinuity of the extrapolated pair potentials at the SN interface for various reasons, to be discussed below. With $0<B\leqslant 1$, one may write at the interface

$$y_1=Bf_1. \tag{16}$$

The current density J in mks units in the one-dimensional S and N regions is

$$J=\frac{\phi_0}{2\pi\mu_0\lambda_s^2|\xi_n|}\frac{m_s}{m_n}\frac{n_n}{n_s}\frac{\chi_{Gn}}{\chi_{Gs}}I. \tag{17}$$

J is the critical current if I has ascertained its largest value. It is then the object to find at a fixed temperature $I_{\max}\equiv I_c$. Since both the S and N regions are ''dirty'' metals ($l_n\approx 33$ nm and $l_s\approx 6$ nm)[10] the χ_G's and other relevant parameters become

$$\chi_{Gs}=1.33l_s/\xi_0,$$

$$\chi_{Gn}=0.391(l_n/|\xi_n|)^2, \tag{18}$$

$$\xi_0=0.18\hbar v_{Fs}/kT_c=1.6\ \ \mu\text{m for Al},$$

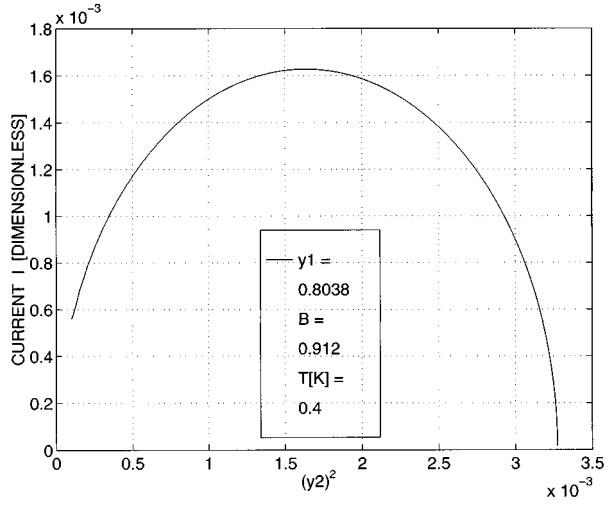

FIG. 2. Solution of Eq. (13) as a function of y_2^2 and I for constant $y_1=0.8038$ for $2|x_1-x_2|=1.48$ μm, corresponding to $B=0.912$ and $T=0.4$ K. Note that the numerical values of y_2^2 and I at the maximum of I are almost the same (see Fig. 5).

$$|\xi_n|=(\hbar v_{Fn} l_n/6\pi kT)^{1/2}=0.136/\sqrt{T}\ \ \mu\text{m for Ag.}$$

Furthermore,

$$\lambda_s^2(T)=\lambda_L^2(0)/[p\chi_{Gs}(1-t^4)]$$

with $p=1/2$, to be consistent with the value of $\lambda_L(0)=16$ nm for Al, which is usually used near $T_c\approx 1.45$ K.[10] The coherence length in the S region is then obtained from the standard relation:

$$\xi_s(T)=\phi_0/[2\pi\sqrt{2}\mu_0 H_c(T)\lambda_s(T)]$$
$$=69.1[(1+t^2)/(1-t^2)]^{1/2}\ \text{nm}$$

with $\mu_0 H_c(T)=10.5(1-t^2)$ mT and $t=T/T_c$.

Although $\xi_s(T)$ and B do not appear explicitly in Eq. (17), ξ_s appears in Eq. (9) and both will be used with the boundary condition (15). For the ''dirty'' limit Eq. (17) reduces to

$$J=\frac{0.391\phi_0}{4\pi\mu_0}\frac{l_n^2}{|\xi_n|^3}\frac{1-t^4}{\lambda_L^2(0)}rI \quad \text{A/m}^2. \tag{19}$$

We used $p=1/2$ as mentioned above, and the ratio $r=(m_s/m_n)(n_n/n_s)=(1.4/1.1)(5.86/18.1)=0.412$ estimated from the specific-heat effective-mass ratio and the free-electron density ratio. Note, the premultiplier of I does not contain the scale factor B of Eq. (16).

In order to solve for the critical current in the N region we consider first Eqs. (13) and (14). At a fixed temperature and fixed half-width of the N region $|x_1-x_2|=d_n$, the relation for $y=y_1$ at the NS interface constitutes a surface in function space (y_2,I,y_1). It is then straightforward to find the exact functional relation $I(y_2)$ for a fixed value of y_1. For example, for $y_1=0.8038$ a typical relation between I and y_2^2 is shown in Fig. 2, which shows that the numerical value of I at the maximum is almost equal to y_2^2. This is correct over most of the temperature range (see Fig. 5). It is worth noticing that in Fig. 2 $I\approx I_c\sin[(\pi/2)(y_2^2/I_c)]$ and is akin to one of Josephson's equations. It shows that the minimum of y^2 and the phase difference across the N region are related but different concepts of the same physical phenomena.

In order to find y_1 we use boundary condition (15), which is equivalent to one of the nodal conditions in micronetworks, and Eqs. (9) and (12). At this point we make certain assumptions. In the S region we assume that d^2f/dx^2 is small and f_0 is very close to unity so that from Eq. (6) $i^2\approx 1-f_0^2$. Then Eq. (9) reduces to

$$\xi_s\left(\frac{df^2}{dx}\right)\Bigg|_{x_1}\approx\sqrt{2}f_1(1-f_1^2). \tag{20}$$

Furthermore, when Eq. (12) is applied at the critical current where $I\approx y_2^2$, it reduces to

$$|\xi_n|\left(\frac{dy^2}{dx}\right)\Bigg|_{x_1}\approx\sqrt{2}y_1^2\sqrt{2-y_1^2}\sqrt{1-(y_2/y_1)^4}. \tag{21}$$

With $y_1=Bf_1$, neglecting $(y_2/y_1)^4$ in Eq. (21), boundary condition (15) leads to the solution of f_1 at the critical current:

$$f_1^2\approx\frac{N^2/B^4+1-[1+(2-B^2)N^2/B^4]^{1/2}}{N^2/B^4+B^2}, \tag{22}$$

where

$$N(T)=\frac{m_n}{m_s}\frac{n_s}{n_n}\frac{\chi_{Gs}}{\chi_{Gn}}\frac{|\xi_n|}{\xi_s}.$$

In the ''dirty'' limit $N(T)=8.25(l_s/\xi_0)[|\xi_n(T)|^3/\ l_n^2\xi_s(T)]$. Note that $f_1^2\to 1$ when $T\to 0$, and $f_1^2\to 0$ when $T\to T_c$.

The accuracy of the critical current solution (19) depends on I, which in turn depends on $y_1(=f_1/B)$. Thus boundary condition (15), which leads to Eq. (22), determines the accuracy of the critical current with the assumptions that $(y_2/y_1)^4$ can be neglected with regard to unity, and that $f_0\approx 1$. We shall show below that this is correct over the experimental temperature range.

Concerning boundary condition (16), this author believes that for a *perfect* electrical contact between two similar metals only a small discontinuity of the pair potentials at the NS interface should exist. B should be close to unity assuming ideal conditions. However, electrical contacts may not be ''ideal'' in an experiment and the approximations made in deriving Eq. (22), and inaccuracies of some of the numerical values, may lead to an ''apparent'' discontinuity. In comparing experiment with theory we let B be an adjustable parameter and expect B to be close to unity. We find $B\approx 0.9$, which supports the assumption that for an ideal NS interface B is close to unity.[11]

Figure 3, curve (a), shows the numerical results of Eq. (19) using Eq. (22), with $B=0.912$, assuming that at least one of the Al branches did not make electrical contact with the Ag wire so that the effective distance between the superconducting patches was $2d_n=1.48$ μm. This result compares very favorably with the experimental results down to below 0.1 K (Fig. 4 of Ref. 1). Curve (b) shows the results with $2d_n=0.68$ μm, normalized with $B=0.320$ to the same

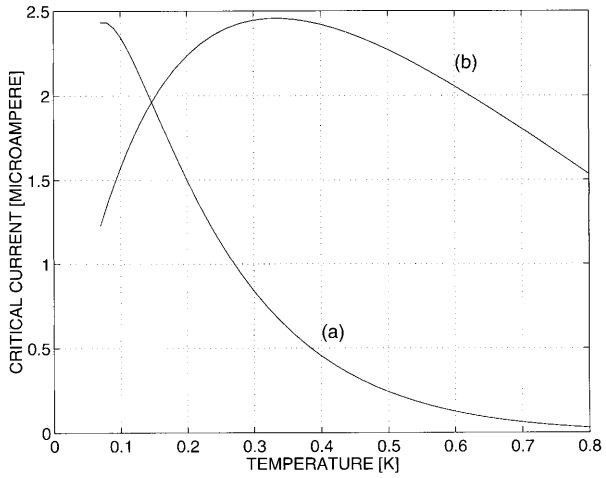

FIG. 3. Solution of Eq. (19) based on f_1 obtained from Eq. (22) for the ''dirty'' S and N limits for (a) $2d_n=1.48$ μm with $B=0.912$, and (b) $2d_n=0.68$ μm with $B=0.320$. The B values were chosen for approximately equal maximum current values of theory and experiment of about 2.5 μA. The cross-sectional area of the silver wire is $w_N e_N=0.21\times0.15$ $(\mu\text{m})^2$. There is very good agreement of curve (a) with the experiment (Fig. 4 of Ref. 1).

maximum value as curve (a). The disagreement with the experimental results is unquestionable.

The accuracy of the numerical results depends on the assumption that $(y_2/y_1)^4 \ll 1$ and that I/y_2^2 at the critical current is approximately unity. Figure 4 shows a plot of $(y_2/y_1)^2$ at the critical current as a function of temperature. It shows that neglecting $(y_2/y_1)^4$ in Eq. (21) introduces an error in the slope of y at the interface of less than 1% over the experimental temperature range down to about 0.07 K.

Similarly, Fig. 5 shows that (I/y_2^2) at $I=I_c$ is close to unity over most of the temperature range, and Fig. 6 shows the normalized critical current I as a function of temperature. Furthermore, $2\xi_s(0)$ and $2\lambda_s(0)$ are only somewhat larger than the width of the Al branches. This could make the assumption that f_0 is close to unity in Eq. (20) inaccurate. This, perhaps, could be hidden by adjusting the value of B. Similarly, inaccuracies in the premultiplier of I of Eq. (19) and in the cross-sectional area of the wire are probably taken care of by adjusting B. In spite of that, it turns out that the value of B is close to unity. The boundary conditions as used here are consistent with those used for micronetworks[9] and also found experimentally[12] for the proximity effect in large magnetic fields. A value of B close to unity supports credence that the theory as presented here is correct, useful and compatible with Zaĭtsev's transmission coefficient[11] $D=4b/(1+b)^2$. With $b=p_{Fn}/p_{Fs}=(1.1/1.4)(1.39/2.03)$ the value of $D\approx0.91$.

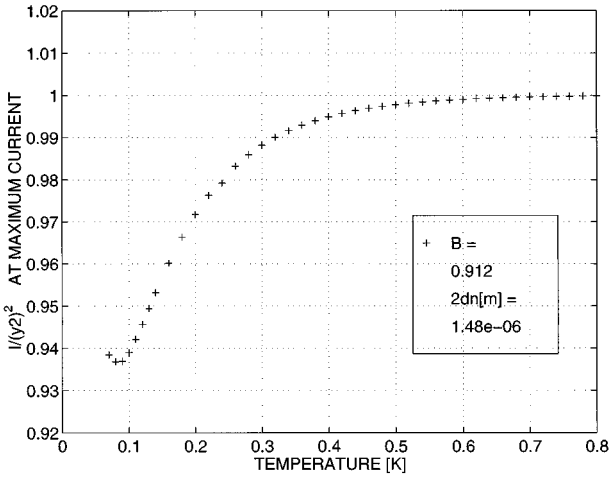

FIG. 5. The ratio of (I/y_2^2) at maximum I as a function of temperature, justifying the assumption $I\approx y_2^2$ at the critical current for an approximate solution, as was used in Ref. 4 for $2d_n/|\xi_n|\gtrsim3$.

Curve (a) of Fig. 3, when calculated with $B=1$, is practically identical to that shown (with $B=0.912$) provided the current is scaled by 0.8. An error of 10% in the measured[10] linear dimensions of the cross section is compatible with $B=1$.

Concerning the current near $T=0$ K we conjecture the following. One expects intuitively that the critical current is finite when $T\to0$ K and not zero as Eq. (19) indicates due to

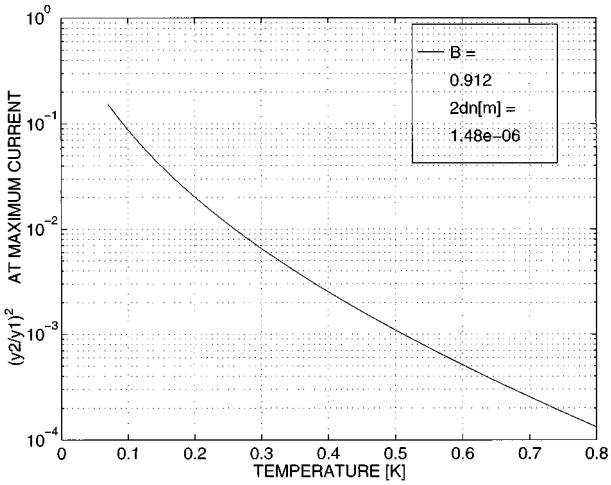

FIG. 4. Plot of $(y_2/y_1)^2$ at maximum I as a function of temperature. Neglecting $(y_2/y_1)^4$ in Eq. (21) causes an error of less than 1% in Eq. (21) for temperatures above 0.07 K.

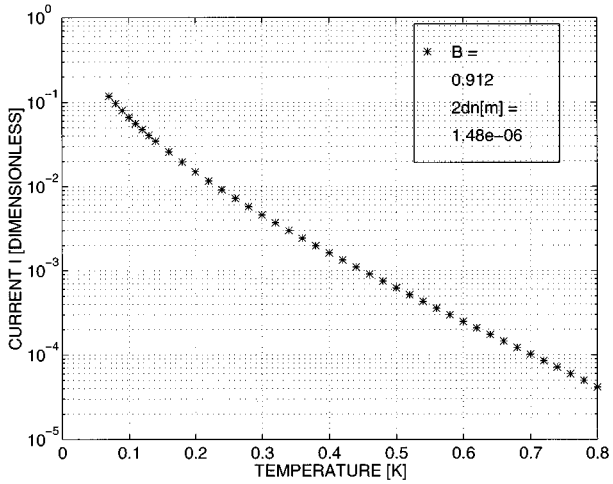

FIG. 6. Solution of the normalized critical current density I in the N region as a function of temperature for the same data as used in Figs. 2–5 with $2d_n=1.48$ μm.

the fact that $|\xi_n| \to \infty$ when $T \to 0$ K. However, Eq. (19) applies only as long as $2d_n \gtrsim 3|\xi_n|$. When $d_n < 1.5|\xi_n|$ the characteristic length over which superconductivity extends is limited not by $|\xi_n|$ but d_n, so that at the low-temperature end where d_n is small compared to $|\xi_n|$, the value of $|\xi_n|$ has to be replaced[13] by about $0.7d_n$ in Eq. (19). Applying this concept to Fig. 3 means that the critical current to the left of the peaks of curves (a) and (b) is practically temperature independent.

The current of Eq. (19) is approximately proportional to $(2d_n/|\xi_n|)^3 \exp(-2d_n/|\xi_n|)$ at the low-temperature end. This leads to a maximum current when $d_n = 1.5|\xi_n(T_s)|$ corresponding to the temperature T_s at which size effects have to be taken into account. Equation (19) then becomes for $T = T_s$ (neglecting t^4)

$$J_s S R_n \approx 0.175 \frac{\pi}{2e} k T_s = 2.37 \times 10^{-5} T_s \ [volt], \qquad (23)$$

where S is the cross-sectional area of the silver wire and R_n is the Drude resistance. With $2d_n = 1.48$ μm the saturation temperature $T_s = 0.076$ K and $J_s S R_n = 1.8$ μV, in good agreement with the experiment of 1.7 μV.

At this point we shall compare the results of the present work with the equation used in Ref. 1 in connection with the interpretation of the experimental data and with other recent theoretical attempts.[14,15] Equation (19) can be cast into the following form:

$$J S R_n = 1.17 \frac{\pi}{2e} k T \frac{2d_n}{|\xi_n|} (1 - t^4) I \ [volt]. \qquad (24)$$

The normalized (dimensionless) current I depends on the boundary value f_1^2, thus on the superconducting properties of the aluminum branches, the ultimate source of superconductivity in the N wire. Reference 1 uses, in the present notation, the following equation taken from Ref. 2:

$$J S R_n = \frac{\pi}{2e} \Delta \frac{2d_n/|\xi_n|}{\sinh(2d_n/|\xi_n|)} \ [volt], \qquad (25)$$

where Δ is interpreted as being the energy gap of aluminum $2\Delta(0)$ such that $(\pi/2e)\Delta \approx 540$ μV. Since the temperature dependence of the maximum value of I in Eq. (24) for temperatures near T_s is roughly the same as $[\sinh(2d_n/|\xi_n|)]^{-1}$, the main difference between Eqs. (24) and (25) is the thermal energy term kT compared to the energy gap of the superconductor. Near the saturation temperature the numerical value of Eq. (25) is about two orders of magnitude larger than Eq. (24) and the overall temperature dependences are different. As mentioned above, Yamafuji *et al.*[3] have pointed out some of the difficulties with the boundary conditions of Ref (2).

Recent work by Wilhelm *et al.*[14] leads to

$$J S R_n \approx 22 \frac{\pi}{2e} k T \frac{2d_n}{|\xi_n|} \exp\left(-\frac{2d_n}{|\xi_n|}\right) \ [volt]. \qquad (26)$$

We use here the same notation as above. Equation (26) has a premultiplier which is one order of magnitude larger than Eq. (24). This is not an essential discrepancy if we consider only the slope of the critical current as a function of temperature above the saturation (size effect) temperature. The latter is similar to that of Eq. (24) near T_s. However, the lack of boundary conditions and/or of any fundamental parameters of the superconductor in Eq. (26) is somewhat puzzling. Furthermore, Eq. (26) is identical to Eq. (15) of Zaikin and Zharkov[15] except that the premultiplier of Eq. (26) is smaller by a factor of 2.

The present and past[4,5] work is based on the Ginzburg-Landau theory which is known to extend empirically to much lower temperatures than expected. The usual argument is that the GL theory holds strictly near the transition temperature. However, since the temperature range of the experiment under consideration is below $T_c/2$, we expect only small temperature variations of the characteristic lengths of the intrinsic superconductor. As we go to lower temperatures, we approach the transition temperature of the N metal, and might be inclined to conjecture, as far as the N metal is concerned, that the accuracy of the theory should become better. As $|\xi_n|$ becomes large, however, size effects must be taken into account.

In conclusion, it is possible that one of the superconducting cells was longer than anticipated.[16] The longest cell is the bottleneck in an experiment. Once the critical current is exceeded, Ohmic heating will drive all of the wire into the normal state. The theory can be fitted to the experiment if one of the assumed cell dimensions is increased by a factor of approximately 2. At low temperatures where the length of a cell becomes comparable to $|\xi_n|$, size effects occur when $2d_n \approx 3|\xi_n|$ and the extent of the induced superconducting domain in the N metal is confined by the dimension of the cell. Below this temperature the critical current saturates.

Discussions with J. Clarke and S. B. Haley are acknowledged. I am grateful to H. Courtois for correspondence.

[1] H. Courtois, Ph. Gandit, and B. Pannetier, Phys. Rev. B **52**, 1162 (1995).

[2] P. G. de Gennes, Rev. Mod. Phys. **36**, 225 (1964).

[3] K. Yamafuji, T. Ezaki, and T. Matsushita, J. Phys. Soc. Jpn. **30**, 965 (1971).

[4] H. J. Fink, Phys. Rev. B **14**, 1028 (1976).

[5] H. J. Fink and R. S. Poulsen, Phys. Rev. B **19**, 5716 (1979).

[6] J. Clarke, Proc. R. Soc. London, Ser. A **308**, 447 (1969).

[7] L. P. Gor'kov, Zh. Eksp. Teor. Fiz. **37**, 1407 (1959) [Sov. Phys. JETP **10**, 998 (1960)].

[8] C. Caroli, P. G. de Gennes, and J. Matricon, Phys. Kondens. Mater. **1**, 176 (1963).

[9] H. J. Fink and V. Grünfeld, Phys. Rev. B **31**, 600 (1985).

[10] H. Courtois (private communication).

[11] A. V. Zaĭtsev, Sov. Phys. JETP **59**, 1015 (1984).

[12] H. J. Fink, M. Sheikholeslam, A. Gilabert, J. P. Laheurte, J. P. Romagnan, J. C. Noiray, and E. Guyon, Phys. Rev. B **14**, 1052 (1976).

[13] This is, for example, similar to the supercooling field of a film which is proportional to λ/ξ for $d \gg \xi$, and proportional to λ/d

for $d/\xi \lesssim 1.7$ [see, e.g., H. J. Fink, D. S. McLachlan, and B. Rothberg-Bibby, in *Progress in Low Temperature Physics* (North-Holland, Amsterdam, 1978), Vol. VIIb, pp. 434–516].

[14] F. K. Wilhelm, A. D. Zaikin, and G. Schön, Czech. J. Phys. **46**, 2395 (1996); J. Low Temp. Phys. **106**, 305 (1997).

[15] A. D. Zaikin and G. F. Zharkov, Sov. J. Low Temp. Phys. **7**, 184 (1984).

[16] Preliminary results of specimens 13 and 14 show similar discrepancies.